Surface Science 602 (2008) 2305–2310

Contents lists available at ScienceDirect

Surface Science

journal homepage: www.elsevier.com/locate/susc

Micropatterning of gold substrates based on poly(propylene sulfide-*bl*-ethylene glycol), (PPS–PEG) background passivation and the molecular-assembly patterning by lift-off (MAPL) technique

L. Feller [a], J.P. Bearinger [b,*], L. Wu [c], J.A. Hubbell [d], M. Textor [a], S. Tosatti [a]

[a] *BioInterface Group, Laboratory for Surface Science and Technology, Swiss Federal Institute of Technology (ETH), Zurich, Switzerland*
[b] *Applied Physics and Biophysics, 7000 East Avenue, L-211, Lawrence Livermore National Laboratory, Livermore, CA 94550, USA*
[c] *Chemistry, Materials, Earth, and Life Sciences, Lawrence Livermore National Laboratory, Livermore, CA 94550, USA*
[d] *Integrative Biosciences Institute and Institute for Chemical Science and Engineering, Ecole Polytechnique Fédérale de Lausanne, Lausanne, Switzerland*

ARTICLE INFO

Article history:
Received 26 February 2008
Accepted for publication 9 May 2008
Available online 16 May 2008

Keywords:
Biosensing
Photolithography
ToF-SIMS
Surface plasmon techniques
Adsorption
Patterning
Self-assembly
Gold

ABSTRACT

Poly(propylene sulfide-*bl*-ethylene glycol) (PPS–PEG) is an amphiphilic block copolymer that spontaneously adsorbs onto gold from solution. This results in the formation of a stable polymeric layer that renders the surface protein-resistant when an appropriate architecture is chosen. The established molecular-assembly patterning by lift-off (MAPL) technique can convert a prestructured resist film into a pattern of biointeractive chemistry and a non-interactive background. Employing the MAPL technique, we produced a micron-scale PPS–PEG pattern on a gold substrate, and then characterized the patterned structure with time-of-flight secondary ion mass spectrometry (ToF-SIMS) and atomic force microscopy (AFM). Subsequent exposure of the PPS–PEG/gold pattern to protein adsorption (full human serum) was monitored *in situ*; SPR-imaging (i-SPR) shows a selective adsorption of proteins on gold, but not on PPS–PEG areas. Analysis shows a reduction of serum adsorption up to 93% on the PPS–PEG areas as compared to gold, in good agreement with previous analysis of homogenously adsorbed PPS–PEG on gold. MAPL patterning of PPS–PEG block copolymers is straightforward, versatile and reproducible, and may be incorporated into biosensor-based surface analysis methods.

© 2008 Elsevier B.V. All rights reserved.

1. Introduction

The lab-on-a-chip modality of a single sensor comprised of numerous chemical functionalities allows for immobilization and analysis of complex molecules [1–3]. Design and quality of the chip surface are essential for performance. High signal-to-noise ratios require (1) a non-interactive background and (2) high affinity towards captured molecules. Quantification of the transducer signal further depends on the quality of arrayed spots. Patterning surfaces and then spotting individual recognition units (multiplexing chemistry) is a way to produce small, information rich chips.

The adsorption of proteins on surfaces is a central concern in sensors and devices that contact biological fluids. Poly(ethylene glycol) (PEG) has been used in numerous biomedically relevant systems to control protein adsorption on surfaces; see [4–6] for a brief overview of documented systems. A previous study of patterning methods of one of these chemistries, PLL-*g*-PEG, and the ensuing long term stability was performed by Lussi et al. [7]. The strength of the interaction between the passivating molecule and the substrate determined the stability of the system. In this case, strong, multidentate interactions between a polymer and the underlying substrate improve coating stability.

Gold surfaces, in particular, are widely used for bioanalytic devices, especially those based on surface plasmon resonance (SPR) methods. The conductivity, resistance to oxidation, and simplicity to produce thin and ultra flat films of gold on other inorganic substrates make this material particularly attractive.

Thiol and thioether containing species are known to chemisorb onto gold, spontaneously forming self-assembled monolayers (SAMs) [8,9]. The application of SAM patterning [10] and SPR [11,12] was previously reported in the literature; Kanda et al. demonstrated the fabrication of arrays with 64 spots on an ethylene-glycol-terminated SAM background [13]. Limitation of such systems lies in the relatively poor stability of chemisorbed alkanethiolates. Indeed, it has been shown that under ambient conditions substantial oxidation and subsequent loss of stability of alkanethiol SAMs takes place within days and the integrity of the adlayer is readily compromised [14–16]. As an alternative to thiol and thioether self-assembled monolayers, we have recently described chemisorption of a poly(propylene sulfide-*bl*-ethylene glycol) (PPS–PEG) triblock copolymer [6]. This copolymer

* Corresponding author. Tel.: +1 925 423 0321; fax: +1 925 424 2778.
E-mail address: bearinger1@llnl.gov (J.P. Bearinger).

0039-6028/$ - see front matter © 2008 Elsevier B.V. All rights reserved.
doi:10.1016/j.susc.2008.05.010

demonstrated high stability as an assembled monolayer on gold, based on the availability of many chemisorption sites per adsorbate molecule as well as higher stability to oxidation of the sulfur in the thioether backbone (as compared to thiolates). In this way, PPS–PEG is analogous to PLL-*g*-PEG, but is applied to gold as opposed to anionic substrates. A number of defined architectures of PPS–PEG have been synthesized and adsorbed from methanol onto gold. Results obtained with human serum albumin (HSA) and serum (HS) indicated a close relationship between protein adsorption resistance and polymer architecture; symmetric triblocks of PPS–PEG with molecular weight of 5k/4k/5k and 2k/4k/2k were the most efficient in reducing protein resistance [17].

Commonly used protein patterning techniques include microcontact printing [1,18–20] and photolithography [21,22]. We modified the molecular-assembly patterning by lift-off (MAPL) process documented by Falconnet [23], to accomplish our goals employing PPS–PEG. MAPL is based on the use of the photoresist itself as the mask for localized surface functionalization; this is similar to previously reported results [22], but the patterned chemistry of interest in this case is not covalently attached. In the first MAPL process documented, a photoresist pattern was transferred into a biochemical pattern by means of spontaneous adsorption of a polycationic poly(ethylene glycol) graft polymer and subsequent photoresist lift-off. The process involves three basic steps: deposition and patterning of a photosensitive polymer (photoresist) on a substrate, assembly of a molecular system and removal of the photoresist and excess material, resulting in a pattern of the assembled molecule on a bare substrate background. Pattern of both micro- and nanometer dimensions have been successfully prepared by this patterning method [23,24]. The technique has been documented for niobia as the substrate with a pattern of a positive photoresist (Shipley S1818), where the pattern is transferred into functionalized poly(L-lysine)-graft-poly(ethylene glycol), PLL-*g*-PEG/PEG-X (X = biotin or cell adhesive peptide), and then backfilled with non-functionalized polymers from aqueous solutions.

SPR-imaging (i-SPR) is a label-free technique that can be employed to read microarrays [13,25–29]. SPR is a common tool in bioanalytical chemistry; biomolecular interactions can be detected in real time with no labelling. SPR microscopy or i-SPR provides the same advantages as SPR spectroscopy with the added feature of monitoring the adsorption with a spatial resolution down to a few microns on the sensing surface. The only modification of the spectroscopy system is replacement of the photodiode detector with a CCD camera. When adsorption of a molecule with a different refractive index than the solution takes place, the presence can be detected in a spatially resolved way by monitoring changes in reflected light intensity. These changes in reflected light intensity are proportional to the change in the refractive index near the surface at an angle near the SPR resonance angle, and can therefore be used for a semi-quantitative analysis of the protein resistance/adsorption of proteins on the surface.

MAPL patterning was adapted to the PPS–PEG block copolymer requirements and patterned substrates were characterized with ToF-SIMS and AFM. Patterned PPS–PEG gold substrates were then tested for protein resistance with i-SPR. Chemical backfilling of patterned surfaces was also explored and characterized with AFM.

2. Materials and methods

2.1. Materials

All solvents were purchased from Fluka (Buchs, Switzerland) and used as received.

Symmetric triblock poly(propylene sulfide)-*block*-poly(ethylene glycol) (Fig. 1) copolymers with a PPS backbone of 3.9 kDa molecular weight and two PEG end chains of 2 kDa were synthesized and characterized as described elsewhere [17,30]. The copolymers were added to methanol at a concentration of 1 mg/ml and sonicated for a few seconds to mix.

Gold layers (47 nm) with an intermediate layer of chromium (1.5 nm) were deposited on glass substrates (10×10 mm or 20×20 mm, Plano GmbH, Germany) using a Leybold direct current magnetron Z600 sputtering unit (PSI, Villigen, Switzerland). Prior to polymer adsorption, the surfaces were cleaned using a UV cleaner (Boekel Ind. Inc., PA, USA) for 30 min.

2.2. Molecular-assembly patterning by lift-off, (MAPL)

The standard MAPL patterning technique [23] was adapted for adsorption of PPS–PEG from aqueous to organic (methanol) solvent. Schematics of the production steps are shown in Fig. 2. We note that our proof-of-concept experiments apply the PPS–PEG to

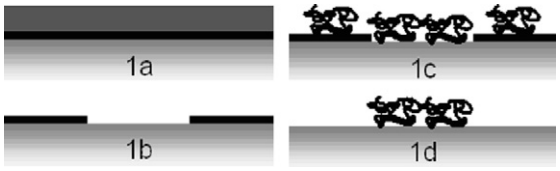

Fig. 2. Schematic of the patterning processing steps employing the MAPL technique. Two positive photoresists (LOR and S1818) are spun coated onto gold substrates (1a). After illumination through a chromium mask, subsequent development and removal of the S1818 by ultrasonication in acetone for 2 min, a sharp pattern of photoresist (LOR) on the gold substrate is revealed (1b). PPS–PEG is adsorbed onto the patterned substrate with a dip-and-rinse process. During this step, the PPS–PEG chemisorbs on the unprotected areas of the gold substrate and physisorbs onto the LOR photoresist (1c). The photoresist is removed by a lift-off resulting in a pattern of PPS–PEG on gold (1d).

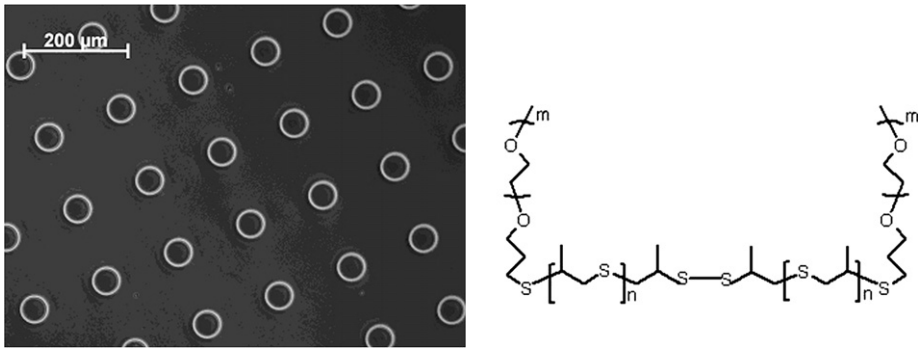

Fig. 1. Left side: Light microscopy image of the mask showing a pattern of both photoresists on a gold substrate. Right side: Chemical structure of a symmetric PPS–PEG triblock copolymer ($m = 44$; $n = 26$).

the spot regions, as opposed to the background, matrix regions. In an actual biosensing application, we would reverse our masks and apply the PPS–PEG to the matrix and functionalized materials to the spots.

Two positive photoresists were spun coated consecutively onto a 2×2 cm^2 gold substrates (4000 rpm for 40 s after having dried the substrate on a hot plate): LOR resist (Micro Chem, USA) with post baking at 150 °C for 5 min and S1818 (Shipley, USA) with post baking at 100 °C for 1 min. The LOR photoresist is desirable based on process chemical compatibility; we knew that the Shipley photoresist would grant straight walled patterned structures (no undercut). Therefore the two photoresists were used in combination.

The photoresist was illuminated through a chromium mask (Photronics Switzerland) for 8 s with 500 W power mercury lamp (exposure 80 mJ/cm^2) and subsequently developed in 1:1 water/microposit 351 developer for 1 min with gentle shaking. S1818 was removed with 2 min ultrasonication in acetone, rinsed with the same solvent and dried with filtered nitrogen. Substrates were then rinsed in a water bath and finally dried with nitrogen.

The gold substrates, containing a patterned LOR were then dipped in a 1 mg/ml solution of PPS–PEG in methanol, rinsed with methanol after 45 min and dried with filtered nitrogen. The lift-off step was done in the following way: LOR was removed by soaking the substrate for 20 s in 1:2 *N*-methyl-pyrolidone (NMP for peptide synthesis, Fluka, Switzerland): ultrapure water and then for 10 s in only ultrapure water. Each sample was then placed vertically in a piranha-cleaned glass container with 10 ml NMP for 6 min in an ultrasonic bath. After 30 s, half of the volume of NMP was replaced with fresh NMP. After 1 min the sample was transferred to a fresh piranha-cleaned NMP containing glass. Finally, the sample was dipped in a glass container containing 1:1 NMP: water before being washed in an ultrapure water bath for 5 min and dried with filtered nitrogen. This modified MAPL process leads to a pattern of PPS–PEG on gold. Bare gold regions then can be further modified with a second applicable chemistry.

2.3. Surface characterization techniques

2.3.1. Light microscopy

The spatial fidelity of the photoresist was characterized by light microscopy (Zeiss Imager M1m, Switzerland) in epi-brightfield mode (reflection) with a 10× objective for the patterned photoresist on the gold substrates.

2.3.2. Variable angle spectrometric ellipsometry (VASE)

Ellipsometric data were measured with a variable angle spectrometric ellipsometer M-2000F (L.O.T. Oriel GmbH, Darmstadt, Germany). The measurement was conducted in the spectral range of 370–1000 nm at three angles of incidence (65°, 70°, and 75°) under ambient conditions. VASE measurements were fitted with multilayer models using WVASE32 analysis software. The analysis of optical constants was based on a bulk gold layer, fitted for *n* and

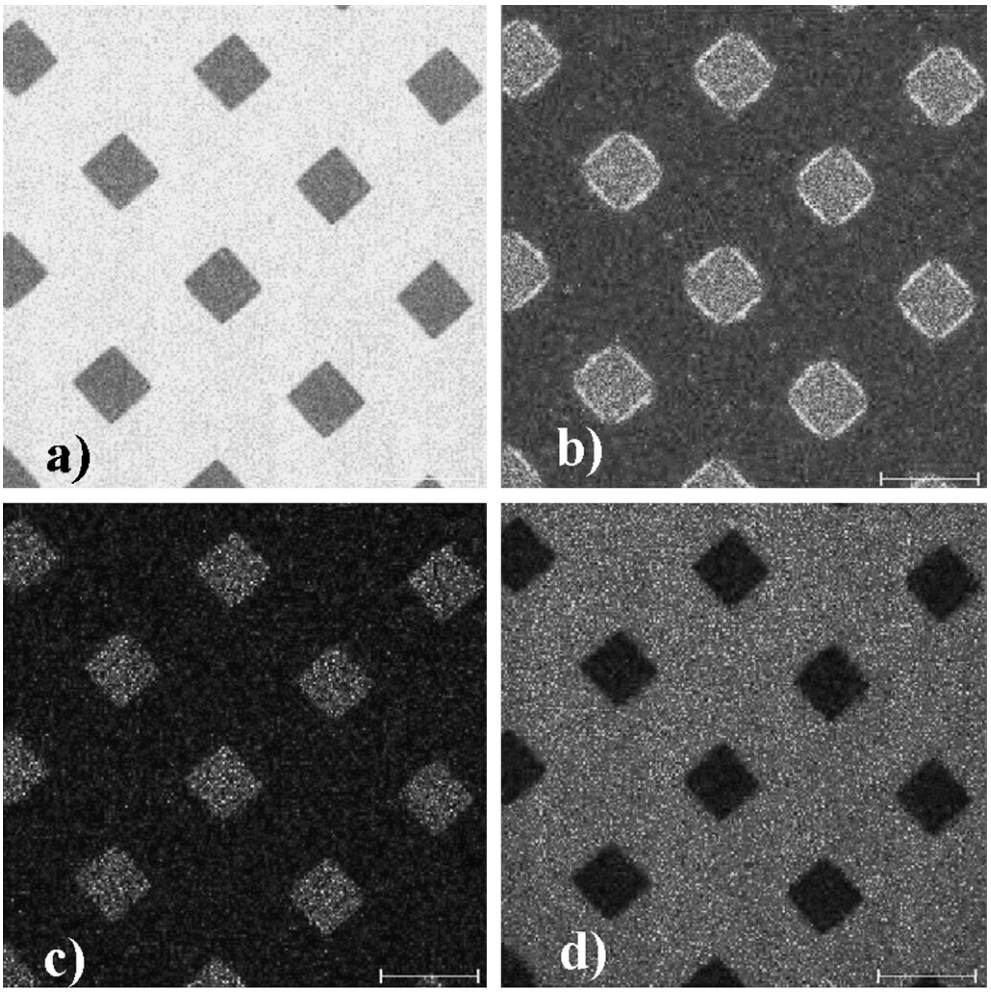

Fig. 3. ToF-SIMS mapping of surface chemistry for a MAPL surface of PPS–PEG adsorbed to 60 μm × 60 μm squares on a gold background. (a) Sum of positive ion intensities (total counts). (b) Intensities representing C_2H_5O (m/q = 45), a typical fragment of PEG. (c) Intensities representing C_3H_6S (m/q = 74), a typical fragment of PPS. (d) Intensities representing gold (m/q = 197). All scale bars are 100 μm.

k on glass. After adsorption of PPS–PEG, the adlayer thickness was determined using a Cauchy model with the approximation for the refractive index of $n = A_n + B_n/\lambda^2 + Cn/\lambda^4$; *where* $A = 1.45$, $B = 0.01$, $C = 0$ [31].

2.3.3. Time-of-flight secondary ion mass spectroscopy (ToF-SIMS)

ToF-SIMS measurements were conducted on a PHI-TRIFT III instrument (Physical Electronics USA, Chanhassen, MN) equipped with a gold (Au) liquid metal ion gun. The ion gun was operated at 22 keV and the primary ion dose was below the static SIMS limit. A bunched mode for high mass resolution was used to acquire mass spectra with a mass resolution $M/\Delta M$ of typically 6000 in both positive and negative spectra. The positive spectra were calibrated using the secondary ion peaks CH_3^+, $C_2H_3^+$, $C_3H_5^+$, the negative spectra using CH^-, OH^-, C_2H^-. After calibration, chemical compositions of secondary ion fragments of interest were identified. Prominent PEG-derived peaks in the positive and negative ion spectra were obtained based on compilations of Wagner et al. [32]; PPS fragments including C_2H_5O and C_3H_6S were also selected for further ToF-SIMS imaging analysis. An un-bunched mode for high image resolution was then used to acquire ToF-SIMS images over an area of $400 \times 400\ \mu m^2$ for 5 min.

2.3.4. Atomic force microscopy (AFM)

A Nanoscope IIIa-MultiMode AFM (Digital Instrument, USA) was used in tapping mode with a Si_3N_4 tip and a 0.12 N/m spring constant. The force was maintained at the lowest possible value by adjusting the set point during imaging. The images were obtained under ambient conditions and height and friction were recorded simultaneously for each point. Scan sizes were between 10 and 20 μm.

2.3.5. Surface plasmon resonance imaging (i-SPR)

The SPR system (Resonant Probes GmbH Goslar, Germany) used a monochromatic laser light source (633 nm) focussed onto a gold-coated glass slide ($n = 1.5230$). Index matching between the 45° prism and the gold-coated glass slide was achieved by using an oil matching the index of the prism ($n_D25 = 1.7000 \pm 0.0002$, Cargille Labs, New Jersey, USA). The instrumental sensitivity measured for methanol was 0.003° with a baseline shift of 0.001°/min prior to PPS–PEG exposure. The experimental sensitivity is 0.03° if one looks at the methanol baseline rinsed with ethanol followed by a return to methanol.

2D information is obtained at a given angle by replacing the detector with a CCD camera [25]. Studies of the relationship between the reflectivity at a fixed angle showed that a range of imaging angles exists in which the reflectivity is linear for refractive index changes and thickness changes [13,33]. Therefore, a semi-quantitative analysis of serum (Roche, Basel, Switzerland) adsorption on samples monitored in the image mode was performed. First, the CCD camera was focused onto the PPS–PEG pattern on the gold substrate in HEPES 2 solution consisting of 10 mM 4-(2-hydroxyethyl) piperazine-1-ethane sulfonic acid and 150 mM NaCl (both from MicroSelect, Fluka Chemie GmbH, Switzerland). An angle scan between 53° and 60° over the whole image as area of interest showed a minimum in light intensity indicating the presence of plasmons. The angle of incidence was fixed to a contrast maximizing angle at 0.4° less than the minimum intensity (56.2°). After a stable baseline was reached and the areas of interests were defined the surface was exposed to full human serum for 30 min followed by rinsing with HEPES 2 buffer.

3. Results and discussion

The MAPL technique, developed by Falconnet [23] could not be applied as originally reported, because the positive photoresist S1818 is soluble in methanol, the solvent of choice for the PPS–PEG adsorption. As an alternative to S1818, LOR photoresist was used. We covered the LOR with S1818 for the photolithographic step, removed the exposed S818 by 2 min ultrasonic immersion in acetone, and then dipped the substrates with the patterned photoresist in the methanol solution. The patterning/processing steps are represented schematically in Fig. 2.

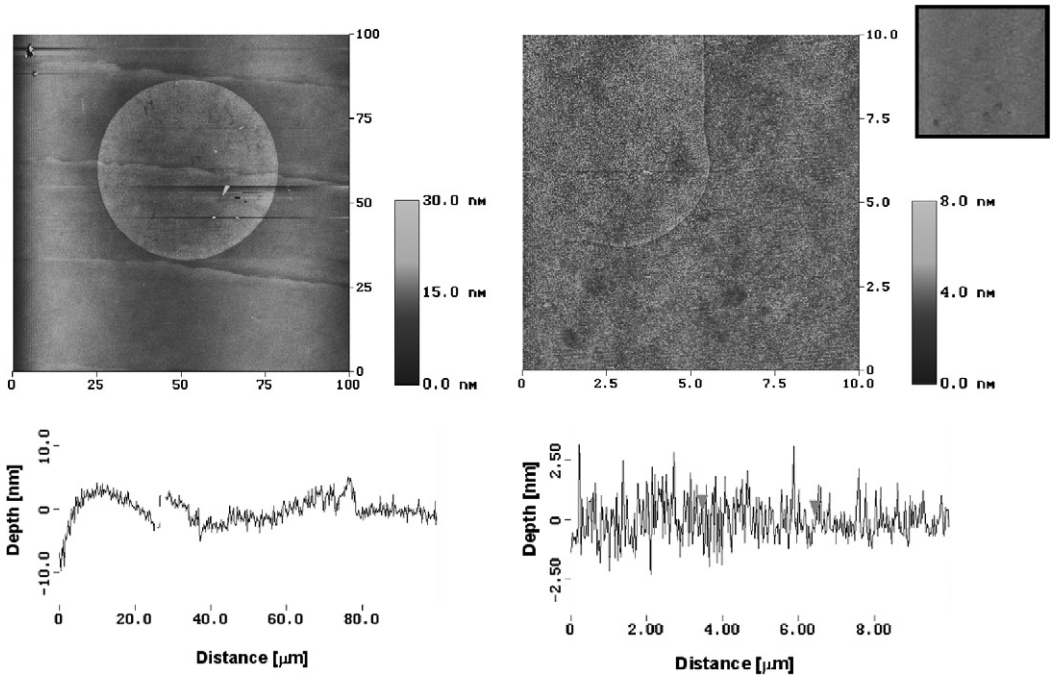

Fig. 4. (left) Tapping mode AFM showing the quality of a PPS–PEG spot on gold background (100 μm). The depth profile shows step heights of the spot corresponding to the layer thickness of homogenous PPS–PEG and discernable edges between the polymer spot and background. (right) Tapping mode AFM of PPS–PEG square spot produced via MAPL technique with subsequent backfill of the same polymer. Spot edge remains detectable although the average height inside and outside of spot is the same. Friction mode shows no difference inside versus outside of the spot (inset) suggesting no chemical contrast in either region.

The light microscopy images showed good quality of the photoresist pattern on the gold substrates (see Fig. 1). In order to quantify the adlayer thickness of the two spin coated photoresist layers, homogenous adlayers on gold substrates were tested for their thickness and quantified with ellipsometry ($n = 3$). The LOR photoresist measured 453 ± 4 nm thick and the S1818 measured 2052 ± 2 nm thick (expected values were 450 nm and 2000 nm, respectively). AFM images (50 μm × 50 μm) of the LOR resist on gold after complete removal of the S1818 photoresist denote a height distance step of 519 nm, which is consistent with the thickness measurements obtained with VASE (data not shown).

3.1. Pattern characterization by ToF-SIMS imaging and atomic force microcopy imaging of PPS–PEG spots on gold substrates

The patterning method was characterized with two highly surface-sensitive analysis techniques: ToF-SIMS and AFM.

Fig. 3 shows ToF-SIMS images of the sum of all ion intensities in the positive ion spectra, the intensities of $C_2H_5O^+$, a characteristic fragment of PEG, the intensities of $C_3H_6S^+$, a characteristic fragment of PPS and the intensity of the gold (a–d). The figure shows ToF-SIMS images of a 60 × 60 μm^2 pattern with higher intensities for fragments related to PPS and PEG in the spots (3b and c) and higher intensities of gold (d) in the background. The gold ion intensity is much lower in the square pattern due to the presence of the PPS–PEG adlayer and the very shallow information depth (≈1–2 nm) characteristic for the static ToF-SIMS technique, which is less than the PPS–PEG adlayer thickness.

AFM imaging in air was used as a complementary surface characterization technique employed to assess the quality of spot definition. Using the AFM to characterize the pattern, one would expect a topographic contrast between the PPS–PEG adlayer and bare gold. The left side of Fig. 4 shows a round spot (50 μm diameter) filled with chemisorbed PPS–PEG on a gold background after complete removal of the positive LOR photoresist. While PPS–PEG chemisorbs to gold as a random coil, in contrast to self-assembling SAMs, the pattern edges of the PPS–PEG on gold (Fig. 4 left) appear sharp and indicate clear contrast between the polymer spot and the background. Furthermore, neither aggregate island formation nor photoresist residue is notable. The layer thickness (4.0 nm) corresponds well with the thickness measured on homogenous PPS–PEG adlayers on gold with the same architecture (3.4 ± 0.4 nm [17]), suggesting that no polymer was removed during the lift-off procedure. Therefore, protein resistance should be maintained. Round spots of 20 μm diameters were reproduced with the same quality. Smaller features can be generated as well [34].

The right part of Fig. 4 indicates an AFM image of PPS–PEG patterned by the MAPL technique after backfill with PPS–PEG. In tapping mode, a rounded square spot front remains detectable, but the surface no longer shows a height difference between the inner and outer regions. Friction mode demonstrates the presence of a homogenous PPS–PEG layer and proves successful molecular backfill.

The modified MAPL approach produced well defined spots on gold substrates. Step heights measured with AFM and chemical mapping with ToF-SIMS reveal a complete and homogenous PPS–PEG adlayer inside the spots on a clean gold background.

3.2. Serum resistance of the MAPL approach characterized with i-SPR

Serum resistance of patterned substrates of PPS–PEG spots on a bare gold background was tested with i-SPR (Fig. 5). We averaged values over three different substrates, with five areas of interest in the PPS–PEG spots and five nearby. We measured intensity changes due to serum exposure of 6.6 ± 4 mV in the spot and 100.5 ± 14 mV on the gold background. A large intensity change corresponds to less serum resistance. Taking the gold background as reference, we measured a serum adsorption reduction of 93% on the PPS–PEG-coated patterns relative to the bare gold background. This finding is in good agreement with previously reported serum adsorption tests on homogenous PPS–PEG adlayers where a corresponding reduction up to 96% was observed [6,17]. This sound agreement in PPS–PEG layer thickness and serum resistance demonstrates that a complete, reproducible, protein-resistant PPS–PEG patterned monolayer was formed.

4. Outlook

Further work will be devoted to the study of alternative patterning approaches, such as photochemical patterning. UV photopatterning is a straightforward method and has been applied to alkanethiolate SAMs by UV irradiation through a mask with micron-scale resolution [35]. This approach has been described for alkanethiols on gold [36], where sulfonate dominated the ToF-SIMS spectra in the area that was exposed to UV radiation. Oxidation of the thiol group results in a strong decrease of the binding strength in comparison to thiolates; alkanethiol SAMs after oxidation can therefore easily be removed by rinsing. Since the chemisorption of PPS–PEG is also depending on Au–S interaction, we hypothesize that this approach will work for our system. Although a more straightforward technique, the main concern with this technique is how to achieve sharp side walls and prevent a gradient of oxidized material from occurring around the edges of masked regions.

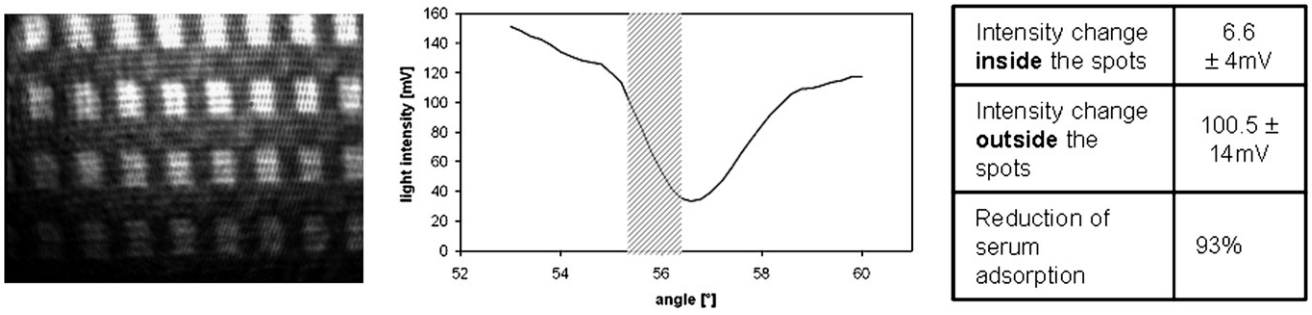

Intensity change **inside** the spots	6.6 ± 4mV
Intensity change **outside** the spots	100.5 ± 14mV
Reduction of serum adsorption	93%

Fig. 5. SPR-imaging of a 60 μm × 60 μm pattern of PPS–PEG spots on gold background in HEPES 2 buffer before serum exposure. An angle scan from 53° to 60° was performed to identify the minimum of the reflected light, which represents the equivalent to the maximal excitation of the plasmons (shown here at 56.6°). Contrast maximizing angle shifts on images from three different substrates averaged 0.4°, so an in coupling angle of 56.2° was chosen for our experiments. Five areas of interest were defined inside different spots containing a PPS–PEG adlayer and additional five areas nearby on the gold background were defined for testing the serum resistance of both surface chemistries at the same time. The table (right) summarizes the changes in light intensities before and after serum exposure collected at an angle of incidence where the change in light intensity is approximately proportional to the adsorption of mass on the area of interest (cross hatched region).

Another strategy would be to use photocatalytical approaches to selectively oxidize PPS–PEG regions [37].

In the context of biomedical device applications of PPS–PEG such as biosensors, polymer adlayer stability is a critical issue in terms of shelf life. While PPS–PEG adlayers on gold surfaces were found to be stable for at least 41 days, alkanethiols SAM were oxidized within 2 weeks of storage under ambient conditions [6]. We believe that PPS–PEG is an attractive platform offering increased stability for gold biochip functionalization in comparison to conventional alkanethiol-based SAMs. Moreover, the combination of PPS–PEG technology and MAPL should allow the creation of patterns with dimensions as low as 100 nm based on earlier work by Falconnet et al. [34].

5. Conclusions

We micropatterned gold substrates with self-assembled PPS–PEG monolayers by adapting the molecular-assembly patterning by lift-off (MAPL) technique. Patterns of different geometries with protein-resistant PPS–PEG adlayers were successfully transferred to gold substrate backgrounds using a photolithographic approach. The PPS–PEG/gold patterns may be backfilled with PPS–PEG polymers functionalized with a (bio)ligand grafted on the end of the PEG chains. Micrometer scale patterning targeted biosensing applications, such as analysis of proteins in an array format the using i-SPR. The approach is label-free and has the potential to maintain the biological activity of desired, adsorbed proteins.

Acknowledgements

We thank Tobias Künzler and Brigitte Städler for assistance with the light microscopy images, and Thomas Blättler and Christoph Huwiler for support with the photolithographic process. The FIRST team and especially Maria Leibinger are acknowledged for access to clean room conditions and support. Thanks to Didier Falconnet for assistance with the MAPL process. Whitney Hartung and Sara Morgenthaler aided the AFM measurements. We gratefully acknowledge funding from NIH R21 EB003991. This work was partially performed under the auspices of the US Department of Energy by Lawrence Livermore National Laboratory under Contract W-7405-Eng-48 and under Contract DE-AC52-07NA27344.

Appendix A. Supplementary data

Supplementary data associated with this article can be found, in the online version, at doi:10.1016/j.susc.2008.05.010.

References

[1] A. Kumar, G.M. Whitesides, Appl. Phys. Lett. 63 (1993) 2002.
[2] D.C. Duffy, R.J. Jackman, K.M. Vaeth, K.F. Jensen, G.M. Whitesides, Adv. Mater. 11 (1999) 546.
[3] J. Ziauddin, D.M. Sabatini, Nature 411 (2001) 107.
[4] G.L. Kenausis, J. Voros, D.L. Elbert, N.P. Huang, R. Hofer, L. Ruiz-Taylor, M. Textor, J.A. Hubbell, N.D. Spencer, J. Phys. Chem. B 104 (2000) 3298.
[5] J.P. Bearinger, D.G. Castner, S.L. Golledge, A. Rezania, S. Hubchak, K.E. Healy, Langmuir 13 (1997) 5175.
[6] J.P. Bearinger, S. Terrettaz, R. Michel, N. Tirelli, H. Vogel, M. Textor, J.A. Hubbell, Nat. Mater. 2 (2003) 259.
[7] J.W. Lussi, D. Falconnet, J.A. Hubbell, M. Textor, G. Csucs, Biomaterials 27 (2006) 2534.
[8] R.G. Nuzzo, D.L. Allara, J. Am. Chem. Soc. 105 (1983) 4481.
[9] J.C.E. Love, L.A. Estroff, J.K. Kriebel, R.G. Nuzzo, G.M. Whitesides, Chem. Rev. (Review) 105 (2005) 1103.
[10] Z. Yang, W. Frey, T. Oliver, A. Chilkoti, Langmuir 16 (2000) 1751.
[11] T. Wink, S.J. van Zuilen, A. Bult, W.P. van Bennekom, The Analyst 122 (1997) 43R.
[12] M. Mrksich, G.B. Sigal, G.M. Whitesides, Langmuir 11 (1995) 4383.
[13] V. Kanda, J.K. Kariuki, D.J. Harrison, M.T. McDermott, Anal. Chem. 76 (2004) 7257.
[14] M. Mrksich, L.E. Dike, J. Tien, D.E. Ingber, G.M. Whitesides, Exp. Cell Res. 235 (1997) 305.
[15] M.J. Tarlov, J.G. Newman, Langmuir 8 (1992) 1398.
[16] M.H. Schoenfisch, J.E. Pemberton, J. Am. Chem. Soc. 120 (1998) 4502.
[17] L.M. Feller, S. Cerritelli, M. Textor, J.A. Hubbell, S.G.P. Tosatti, Macromolecules 38 (2005) 10503.
[18] M. Mrksich, G.M. Whitesides, Trends Biotechnol. 13 (1995) 228.
[19] J. Lahiri, E. Ostuni, G.M. Whitesides, Langmuir 15 (1999) 2055.
[20] G.M. Whitesides, E. Ostuni, S. Takayama, X. Jiang, D.E. Ingber, Annu. Rev. Biomed. Eng. 3 (2001) 335.
[21] C.H. Thomas, J.H. Collier, C.S. Sfeir, K.E. Healy, Proc. Natl. Acad. Sci. USA 99 (2002) 1972.
[22] C.H. Thomas, J.B. Lhoest, D.G. Castner, C.D. McFarland, K.E. Healy, J. Biomech. Eng. – Trans. ASME 121 (1999) 40.
[23] D. Falconnet, A. Koenig, F. Assi, M. Textor, Adv. Funct. Mater. 14 (2004) 749.
[24] D. Falconnet, Molecular assembly patterning by lift-off at the micro- and nanoscale for applications in the biosciences, ETH Zürich, 2005.
[25] J.S. Shumaker-Parry, C.T. Campbell, Anal. Chem. 76 (2004) 907.
[26] R. Rella, J. Spadavecchia, M.G. Manera, P. Siciliano, A. Santino, G. Mita, Biosens. Bioelectron. 20 (2004) 1140.
[27] B.P. Nelson, T.E. Grimsrud, M.R. Liles, R.M. Goodman, R.M. Corn, Anal. Chem. 73 (2001) 1.
[28] G. Steiner, V. Sablinskas, A. Hubner, C. Kuhne, R. Salzer, J. Mol. Struct. 509 (1999) 265.
[29] B. Rothenhausler, W. Knoll, Nature 332 (1988) 615.
[30] A. Napoli, N. Tirelli, G. Kilcher, J.A. Hubbell, Macromolecules 34 (2001) 8913.
[31] E.Palik, Palik, Handbook of Optical Constants of Solids, Academic, New York, Orlando, 1985.
[32] M.S. Wagner, S. Pasche, D.G. Castner, M. Textor, Anal. Chem. 76 (2004) 1483.
[33] T. Wilkop, Z. Wang, Q. Cheng, Langmuir 20 (2004) 11141.
[34] D. Falconnet, D. Pasqui, S. Park, R. Eckert, H. Schift, J. Gobrecht, R. Barbucci, M. Textor, Nano Lett. 4 (2004) 1909.
[35] M.J. Tarlov, D.R.F. Burgess, G. Gillen, J. Am. Chem. Soc. 115 (1993) 5305.
[36] J. Huang, J.C. Hemminger, J. Am. Chem. Soc. 115 (1993) 3342.
[37] J.S. Bearinger, G. Stone, A.T. Christian, L. Dugan, A.L. Hiddessen, K.J. Wu, L. Wu, J. Hamilton, C. Stockton, J.A. Hubbell, Langmuir 24 (2008) 5179.